Influence of Thoracic Endovascular Aortic Repair on True Lumen Helical Morphology for Stanford Type B Dissections

From the Western Vascular Society

Influence of thoracic endovascular aortic repair on true lumen helical morphology for Stanford type B dissections

Johan Bondesson, MS,[a] Ga-Young Suh, PhD,[b,c] Neil Marks,[c] Michael D. Dake, MD,[d] Jason T. Lee, MD,[c] *and* Christopher P. Cheng, PhD,[c] *Gothenburg, Sweden; Long Beach and Stanford, Calif; and Tucson, Ariz*

ABSTRACT

Objective: Thoracic endovascular aortic repair (TEVAR) can change the morphology of the flow lumen in aortic dissections, which may affect aortic hemodynamics and function. This study characterizes how the helical morphology of the true lumen in type B aortic dissections is altered by TEVAR.

Methods: Patients with type B aortic dissection who underwent computed tomography angiography before and after TEVAR were retrospectively reviewed. Images were used to construct three-dimensional stereolithographic surface models of the true lumen and whole aorta using custom software. Stereolithographic models were segmented and co-registered to determine helical morphology of the true lumen with respect to the whole aorta. The true lumen region covered by the endograft was defined based on fiducial markers before and after TEVAR. The helical angle, average helical twist, peak helical twist, and cross-sectional eccentricity, area, and circumference were quantified in this region for pre- and post-TEVAR geometries.

Results: Sixteen patients (61.3 ± 8.0 years; 12.5% female) were treated successfully for type B dissection (5 acute and 11 chronic) with TEVAR and scans before and after TEVAR were retrospectively obtained (follow-up interval 52 ± 91 days). From before to after TEVAR, the true lumen helical angle (−70.0 ± 71.1 to −64.9 ± 75.4°; $P = .782$), average helical twist (−4.1 ± 4.0 to −3.7 ± 3.8°/cm; $P = .674$), and peak helical twist (−13.2 ± 15.2 to −15.4 ± 14.2°/cm; $P = .629$) did not change. However, the true lumen helical radius (1.4 ± 0.5 to 1.0 ± 0.6 cm; $P < .05$) and eccentricity (0.9 ± 0.1 to 0.7 ± 0.1; $P < .05$) decreased, and the cross-sectional area (3.0 ± 1.1 to 5.0 ± 2.0 cm^2; $P < .05$) and circumference (7.1 ± 1.0 to 8.0 ± 1.4 cm; $P < .05$) increased significantly from before to after TEVAR. The distinct bimodal distribution of chiral and achiral native dissections disappeared after TEVAR, and subgroup analyses showed that the true lumen circumference of acute dissections increased with TEVAR, although it did not for chronic dissections.

Conclusions: The unchanged helical angle and average and peak helical twists as a result of TEVAR suggest that the angular positions of the true lumen are constrained and that the endografts were helically conformable in the angular direction. The decrease of helical radius indicated a straightening of the corkscrew shape of the true lumen, and in combination with more circular and expanded lumen cross-sections, TEVAR produced luminal morphology that theoretically allows for lower flow resistance through the endografted portion. The impact of TEVAR on dissection flow lumen morphology and the interaction between endografts and aortic tissue can provide insight for improving device design, implantation technique, and long-term clinical outcomes. (J Vasc Surg 2021;■:1-9.)

Keywords: TEVAR; Thoracic aorta; Type B aortic dissection; True lumen; Helical angle; Helical twist; Helical radius; Cross-sectional eccentricity; Circumference; Cross-sectional area

Thoracic endovascular aortic repair (TEVAR) has shown to be a favorable treatment strategy for Stanford type B dissections owing to short recovery times, and low rates of perioperative complications and early morbidity and mortality.[1-3] Perioperative success of TEVAR is achieved by covering of the intimal tear for

From the Division of Dynamics, Chalmers University of Technology, Gothenburg[a]; the Department of Biomedical Engineering, California State University, Long Beach[b]; the Division of Vascular Surgery, Stanford University, Stanford[c]; and the Department of Surgery, University of Arizona, Tucson.[d]

Author conflict of interest: G.S. and C.C. have received unrestricted research funding from W. L. Gore & Associates, Medtronic, Endologix, and Bentley. G.S. and C.C. performed consulting work for Cordis and Terumo. M.D. is a consultant for W. L. Gore & Associates and Cook Medical. J.B., N.M., and J.L. have nothing to disclose.

Presented at the Thirty-fifth Annual Meeting of the Western Vascular Society, Virtual, September 27-29, 2020.

Additional material for this article may be found online at www.jvascsurg.org.

Correspondence: Johan Bondesson, PhD, Division of Dynamics, Chalmers University of Technology, Hörsalsvägen 7A, 412 96 Gothenburg, Sweden (e-mail: johbond@chalmers.se).

The editors and reviewers of this article have no relevant financial relationships to disclose per the JVS policy that requires reviewers to decline review of any manuscript for which they may have a conflict of interest.

0741-5214

https://doi.org/10.1016/j.jvs.2021.04.029

false lumen depressurization and expansion of the true lumen, with a goal of oversizing the endograft by approximately 10% to ensure a good proximal seal and fixation without applying excessive stress to the tissue.[4] Postoperative success after TEVAR includes increased flow into the true lumen, no endoleak, and false lumen thrombosis incorporated into aortic remodeling. Correct placement based on preoperative geometric features have also been shown to decrease risk for type IA endoleaks.[5]

It has previously been reported that type B aortic dissections show a helical (ie, spiraling) propagation pattern, with a bimodal distribution of the true lumen either being strongly right-handed chiral or achiral.[6] The mechanisms that cause dissection helical morphology and propagation are not fully understood, but are hypothesized to be influenced by the helical blood flow created by the twisting contraction of the left ventricle and helical alignment of microstructural fibers within the layers of the aortic walls.[7,8]

TEVAR endografts possess mechanical stiffness, and thus are expected to affect true lumen morphology and vice versa. The combination of native anatomy and the implanted endograft yields updated mechanical properties and hemodynamic conditions, affecting physiology, flow resistance, and remodeling. Quantification of how TEVAR affects dissection helical morphology could have several benefits: (1) preoperative planning, (2) postoperative evaluation, and (3) improvement of endograft design and implantation strategy. We introduce a method to characterize true lumen helical morphology and its alteration owing to TEVAR, using longitudinally resolved helical metrics quantified before and after TEVAR.

ARTICLE HIGHLIGHTS

- **Type of Research:** Single-center retrospective cohort study
- **Key Findings:** In 16 patients with type B aortic dissection treated with thoracic endovascular aortic repair (TEVAR), the helical radius and true lumen eccentricity decreased significantly, whereas the true lumen cross-sectional area and circumference increased significantly. The helical angle, average helical twist, and peak helical twist remained unaltered. The distinct grouping based on helical chirality TEVAR vanished after TEVAR.
- **Take Home Message:** TEVAR changes the shape of the true lumen by making the cross-sectional shape more circular and larger in size, which in its turn yields a straighter true lumen corkscrew centerline. From a geometric point of view, these changes altogether yields an improved luminal shape allowing for lower flow resistance. Right-handed chiral (spiraling) dissections can in some cases become achiral after TEVAR.

METHODS

Patient cohort, image acquisition, and modeling. Patients with chronic or acute Stanford type B dissection who had been treated with TEVAR were retrospectively included in this study.[9-12] All patients gave informed consent and the study was approved by the institutional review board. This study performed visual screening of patients' computed tomography angiography (CTA) data, and included those with distinct separation of true and false lumen with dissection length exceeding 5 cm. Additionally, patients with Marfan syndrome were excluded to ensure that aortic wall properties were comparable.

All patients had undergone pre- and post-TEVAR CTA, and the images were processed using open-source software SimVascular to construct three-dimensional stereolithographic surface models for the (1) true lumen, (2) whole aorta defined by the outer aortic wall, (3) endograft (post-TEVAR only), and (4) arch branches, including the brachiocephalic, left common carotid, and left subclavian arteries.[13] Pre- and post-TEVAR volume-rendered CTAs and surface models for one example patient with chronic dissection are shown in Fig 1.

The surface models of the true lumen and whole aorta were then co-registered and simultaneously segmented using a dual lumen segmentation algorithm.[6,14] By relating the segmented surfaces to a fiducial marker (the branch point of the left common carotid artery [LCCA]), Lagrangian cylindrical coordinates were employed to mathematically represent the aortic and endograft surfaces.[13] A longitudinal guideline originating from the LCCA served as a fiducial curve with which to reference circumferential position.[15,16]

For comparison between the pre- and post-TEVAR states, a region of interest (ROI) was defined consistently using the Lagrangian coordinate system (Fig 1, *C*). To find the proximal limit for the ROI, a longitudinal position 5 cm distal to the LCCA was found in the pre-TEVAR model. Exceptionally, if the intimal tear of the true lumen was located more distally, then the proximal end of the ROI was defined as the position with the intimal tear instead. The intimal tear location was defined where the centerlines of the whole aorta and true lumen diverged by more than 0.1 cm. The same longitudinal position was transferred to the post-TEVAR model, as indicated by the dashed arrows in Fig 1, *C*. Analogously, to define the distal end of the ROI, the centerline distance from the LCCA to the distal end of the endograft was found in the post-TEVAR model, and then applied to the pre-TEVAR model.

Extraction of helical and cross-sectional metrics. Within the defined ROI, a series of true lumen morphology metrics were extracted. True lumen helical

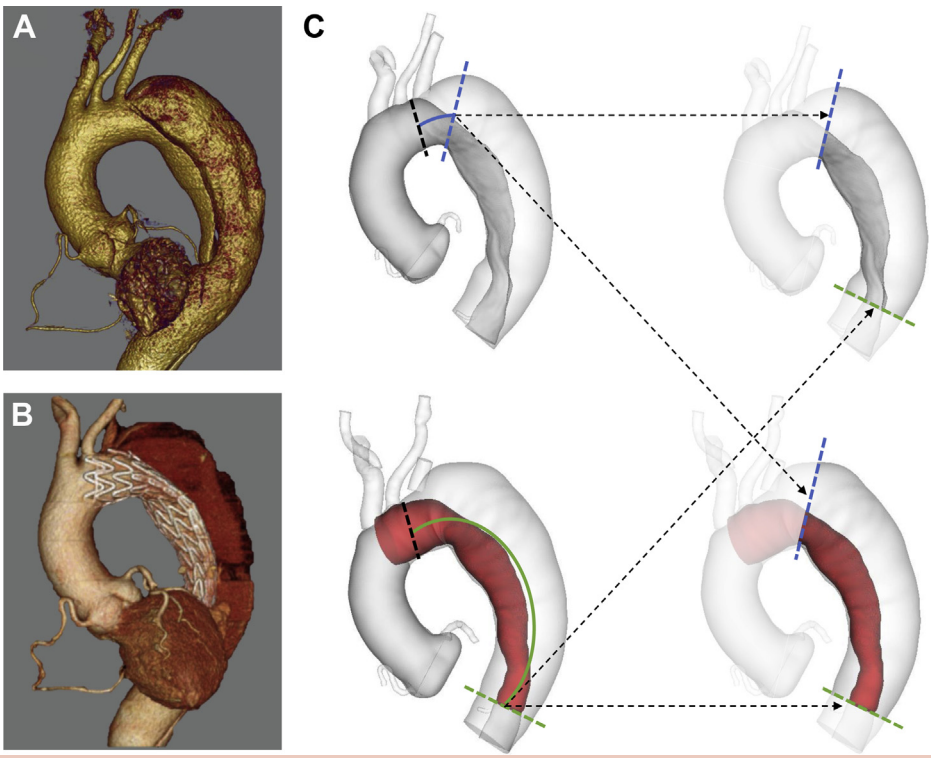

Fig 1. Volume-rendered computed tomography angiography (CTA) of a patient with chiral chronic dissection with **(A)** pre-thoracic endovascular aortic repair (TEVAR) and **(B)** post-TEVAR, and **(C)** geometric surface models of before TEVAR (*top*) and after TEVAR (*bottom*). The models include true lumen (*dark grey*), whole aorta and arch branches (*light grey*), and post-TEVAR endograft (*red*). The dashed arrows indicate how the dissection region of interest (ROI) was found and consistently applied to both pre- and post-TEVAR states **(C)**. The ROI was defined (1) at the proximal end as 5 cm distal to the left common carotid artery (LCCA), or at the intimal tear, whichever was more distal (blue dashed lines), and (2) at the distal end as the distal end of the endograft (green dashed lines) (**C**, right column).

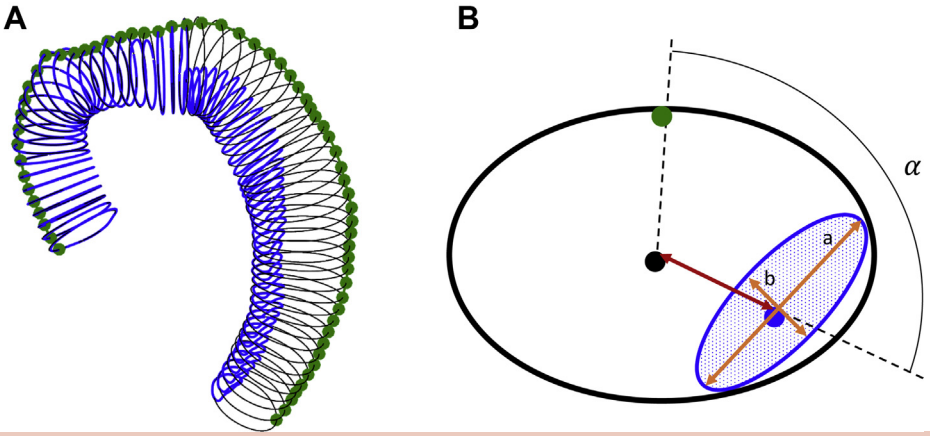

Fig 2. Overview of morphology metric definition. **(A)** Contours of the whole aorta (*black*), true lumen (*blue*), and the longitudinal fiducial marker guideline (*green*). **(B)** Helical angle (α), true lumen area (*dotted blue*), helical radius (*red arrow*), major (a) and minor (b) axes of true lumen (*orange arrows*), and true lumen circumference (*blue line*).

metrics included the (1) helical angle (α), defined as the angle of separation between the centroid of the true lumen and the longitudinal fiducial marker guideline originating from the LCCA (Fig 2), (2) average helical twist defined as the change of helical angle divided by the centerline length of the ROI, and (3) peak helical twist defined as the maximum change of helical angle over a sliding 4-cm span. The sliding span size was set

Table I. Patient information

Patient No.	Age (y)	Sex (M/F)	Dissection type	Chirality type	Prior aortic repair	Follow-up time, days
A1	61	M	Acute	Achiral	–	5
A2	52	M	Acute	Right handed	–	2
A3	58	F	Acute	Achiral	–	4
A4	61	M	Acute	Achiral	Visceral stenting	2
A5	60	M	Acute	Right handed	–	99
C1	69	M	Chronic	Right handed	–	2
C2	57	M	Chronic	Achiral	–	2
C3	65	M	Chronic	Achiral	Ascending aorta	59
C4	82	M	Chronic	Right handed	–	87
C5	57	M	Chronic	Right handed	–	2
C6	63	M	Chronic	Achiral	Ascending and arch	370
C7	58	M	Chronic	Achiral	Ascending aorta	9
C8	58	M	Chronic	Achiral	–	36
C9	72	M	Chronic	Right handed	–	34
C10	59	M	Chronic	Right handed	–	49
C11	48	F	Chronic	Achiral	–	66

F, Female; *M*, male.

according to previous recommendations for quantification of longitudinally varying metrics.[14-16] The helical radius was defined as the distance between the centroids of the whole aorta and the true lumen, as annotated with the red arrow in Fig 2, *B*. True lumen cross-sectional metrics for each contour included cross-sectional: (1) area, (2) circumference, and (3) eccentricity defined as $\varepsilon = \sqrt{1-(\frac{b}{a})^2}$. The major ($a$) and minor axes ($b$) of the true lumen used in this formula are visualized in Fig 2, *B*.

Subgroup analyses. To further understand the TEVAR-induced alterations on true lumen morphology, two subgroup analyses were performed. First, the cohort was divided into chronic and acute subgroups to assess how the level of acuity affected alterations. Second, based on the helical angle within the ROI of the pre-TEVAR models, the cohort was split into two groups: achiral and right-handed chiral based a helical angle threshold of −90°.[6]

Statistics. Two-tailed paired *t* tests were used to compare metrics between the pre- and post-TEVAR states. Two-tailed unpaired *t* tests were used to compare acute vs chronic and achiral vs chiral subgroups. To ensure correct assumptions when performing the unpaired *t* tests, a Bartlett's test was used to check homogeneity of variances.[17] The significance threshold was a *P* of less than .05 for both paired and unpaired *t* tests.

RESULTS

Patient and device information. Sixteen patients (61.3 ± 8.0 years; 12.5% female) treated successfully for type B aortic dissection with TEVAR using C-TAG endografts (W. L. Gore & Associates, Flagstaff, Ariz) were included in this study. For patients where the endograft covered the ostium of the left subclavian artery, the left subclavian artery was occluded with an Amplatzer plug, and flow was achieved via bypass graft from the LCCA. For each patient, completion angiography confirmed no retrograde flow to the false lumen after endograft implantation. The mean and median time to follow up were 51.8 and 21.5 days, respectively (Table I). The cohort comprised of 5 acute vs 11 chronic dissections, and 9 achiral vs 7 right-handed chiral true lumens. Three patients (C3, C6, and C7) had undergone previous surgical repair proximal to the descending aorta.

Alteration of helical metrics. As seen in Table II, although the helical angle (−70.0 ± 71.1 to −64.9 ± 75.4°; $P = .782$), average helical twist (−4.1 ± 4.0 to −3.7 ± 3.8°/cm; $P = .674$), and peak helical twist (−13.2 ± 15.2 to −15.4 ± 14.2°/cm; $P = .629$) did not change significantly from before to after TEVAR, the helical radius decreased significantly for all patients (1.4 ± 0.5 to 1.0 ± 0.6 cm; $P < .05$). Similar to the results for all patients, both acute and chronic dissection subgroups, as well as both achiral and right-handed chiral subgroups, showed an unchanged helical angle, average helical twist, and peak helical twist, but significantly decreased the helical radius as a result of TEVAR (Table II). There were no significant differences in helical metrics between the acute and chronic dissection subgroups before or after TEVAR. The significant differences in helical angle, average helical twist, and peak helical twist between the two chirality-based

Table II. Helical metrics (helical angle, average helical twist, peak helical twist, and average helical radius) and cross-sectional metrics (average true lumen eccentricity, true lumen cross-sectional area, and average true lumen circumference) for the patient cohort and subgroups based on acuity and chirality before and after thoracic endovascular aortic repair (TEVAR)

	Subgrouping basis	Acuity		Chirality	
		All (n = 16)	Acute (n = 5)	Chronic (n = 11)	Achiral (n = 9)	Chiral (n = 7)
Helical metrics						
Helical angle, °	Preoperative	−70.0 ± 71.1	−75.9 ± 71.8	−67.3 ± 74.2	−12.5 ± 15.3[a]	−143.9 ± 31.7[a]
	Postoperative	−64.9 ± 75.4	−41.9 ± 52.3	−75.3 ± 84.0	−35.5 ± 43.9	−102.7 ± 93.2
	P value	.782	.362	.718	.174	.258
Average helical twist, °/cm	Preoperative	−4.1 ± 4.0	−5.5 ± 4.6	−3.4 ± 3.7	−1.1 ± 1.2[a]	−8.0 ± 2.4[a]
	Postoperative	−3.7 ± 3.8	−3.5 ± 3.9	−3.7 ± 4.0	−2.2 ± 2.2	−5.5 ± 4.8
	P value	.674	.379	.761	.156	
Peak helical twist, °/cm	Preoperative	−13.2 ± 15.2	−18.6 ± 16.1	−10.7 ± 14.8	−3.0 ± 7.7[a]	−26.3 ± 11.9[a]
	Postoperative	−15.4 ± 14.2	−8.8 ± 17.3	−18.4 ± 15.8	−10.0 ± 9.7	−22.4 ± 16.7
	P value	.629	.314	.132	.204	.648
Average helical radius, cm	Preoperative	1.4 ± 0.5[b]	1.0 ± 0.4[b]	1.6 ± 0.5[b]	1.5 ± 0.4[b]	1.4 ± 0.7[b]
	Postoperative	1.0 ± 0.6[b]	0.5 ± 0.3[b]	1.3 ± 0.5[b]	1.0 ± 0.5[b]	1.2 ± 0.7[b]
	P value	**<.05**	**<.05**	**<.05**	**<.05**	**<.05**
Cross-sectional metrics						
Average true lumen eccentricity (−)	Preoperative	0.9 ± 0.1[b]	0.8 ± 0.2[b]	0.9 ± 0.1[b]	0.9 ± 0.1[b]	0.8 ± 0.1[b]
	Postoperative	0.7 ± 0.1[b]	0.6 ± 0.1[b]	0.7 ± 0.1[b]	0.7 ± 0.2[b]	0.6 ± 0.2[b]
	P value	**<.05**	**<.05**	**<.05**	**<.05**	**<.05**
Average true lumen area, cm^2	Preoperative	3.0 ± 1.1[b]	3.0 ± 0.9[b]	3.0 ± 1.2[b]	2.6 ± 0.9[b]	3.5 ± 1.2[b]
	Postoperative	5.0 ± 2.0[b]	6.4 ± 2.1[a,b]	4.3 ± 1.6[a,b]	4.5 ± 1.8[b]	5.5 ± 2.1[b]
	P value	**<.05**	**<.05**	**<.05**	**<.05**	**<.05**
Average true lumen circumference, cm	Preoperative	7.1 ± 1.0[b]	7.1 ± 0.9[b]	7.2 ± 1.1	6.9 ± 1.1	7.5 ± 0.9
	Postoperative	8.0 ± 1.4[b]	9.0 ± 1.4[a,b]	7.5 ± 1.2[a]	7.6 ± 1.4	8.4 ± 1.4
	P value	**<.05**	**<.05**	.367	.108	.125

Boldface entries indicate statistical significance.
[a]Significant difference between subgroups based on acuity or chirality.
[b]Significant difference between before and after TEVAR.

subgroups before TEVAR (indicated by [a] in Table II) vanished after TEVAR.

Alteration of cross-sectional metrics. As seen in Table II, true lumen eccentricity (0.9 ± 0.1 to 0.7 ± 0.1; $P < .05$), true lumen cross-sectional area (3.0 ± 1.1 to 5.0 ± 2.0 cm^2; $P < .05$), and true lumen circumference (7.1 ± 1.0 to 8.0 ± 1.4 cm; $P < .05$), were all significantly changed from before to after TEVAR for all patients. These cross-sectional metrics were also significantly altered for the acute subgroup, whereas for the chronic, achiral, and chiral subgroups, only true lumen eccentricity and cross-sectional area were significantly different. Comparing achiral and chiral subgroups, none of the cross-sectional metrics before or after TEVAR were statistically different. The acute and chronic dissection subgroups did not exhibit any differences before TEVAR, but statistical differences were observed for true lumen area and circumference post-TEVAR (indicated by [a] in Table II). Fig 3 shows longitudinal variation of helical angle, helical radius, and cross-sectional metrics for an achiral acute patient (A4) and a chiral chronic patient (C1).

DISCUSSION

The fact that the helical angle, average helical twist, and peak helical twist did not change significantly with TEVAR indicates that the endograft and delivery procedure exhibit high conformability in the angular direction, that is, allowing the true lumen to remain in its native angular orientation without significant uncurling effects, either over the whole length or locally. This has been alluded to previously, with the hypothesis that in chronic dissections the true lumen wall is thickened and restricts major remodeling.[18,19]

Interestingly, although the achiral and right-handed chiral subgroups exhibited significant differences in the pre-TEVAR helical angle, average helical twist, and peak helical twist, those significant differences did not remain after TEVAR. This finding means that, even though the overall data suggest that the endografts in this study

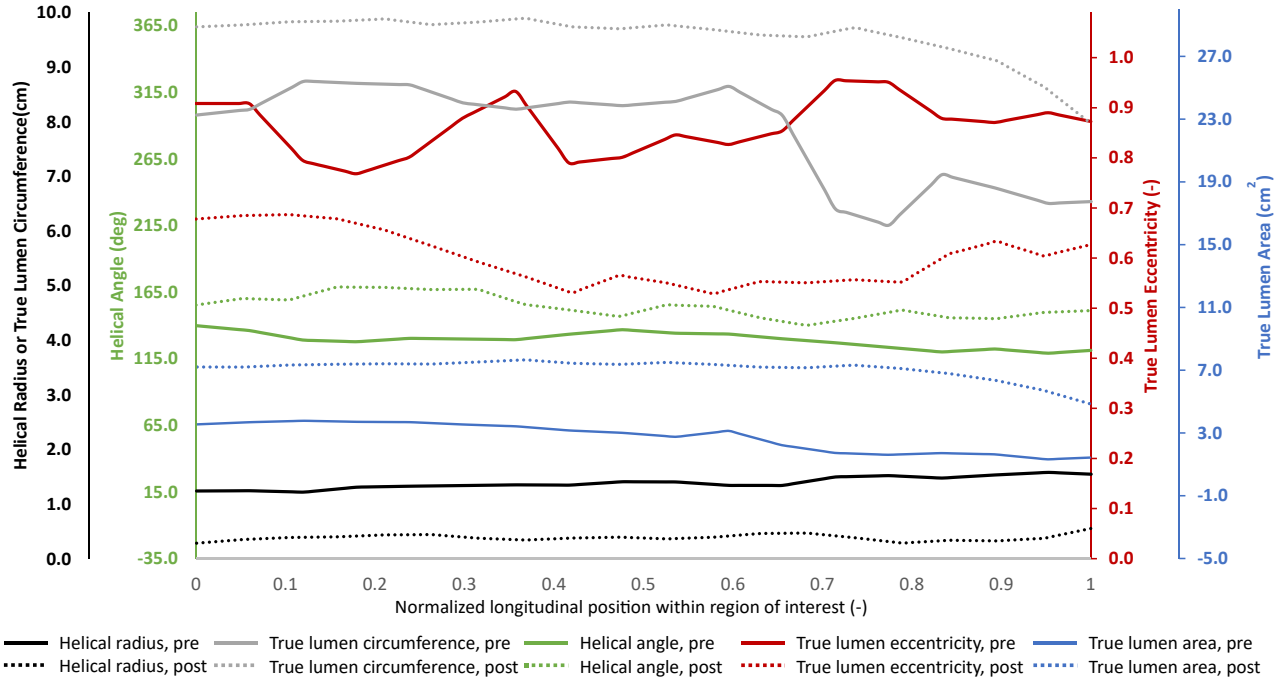

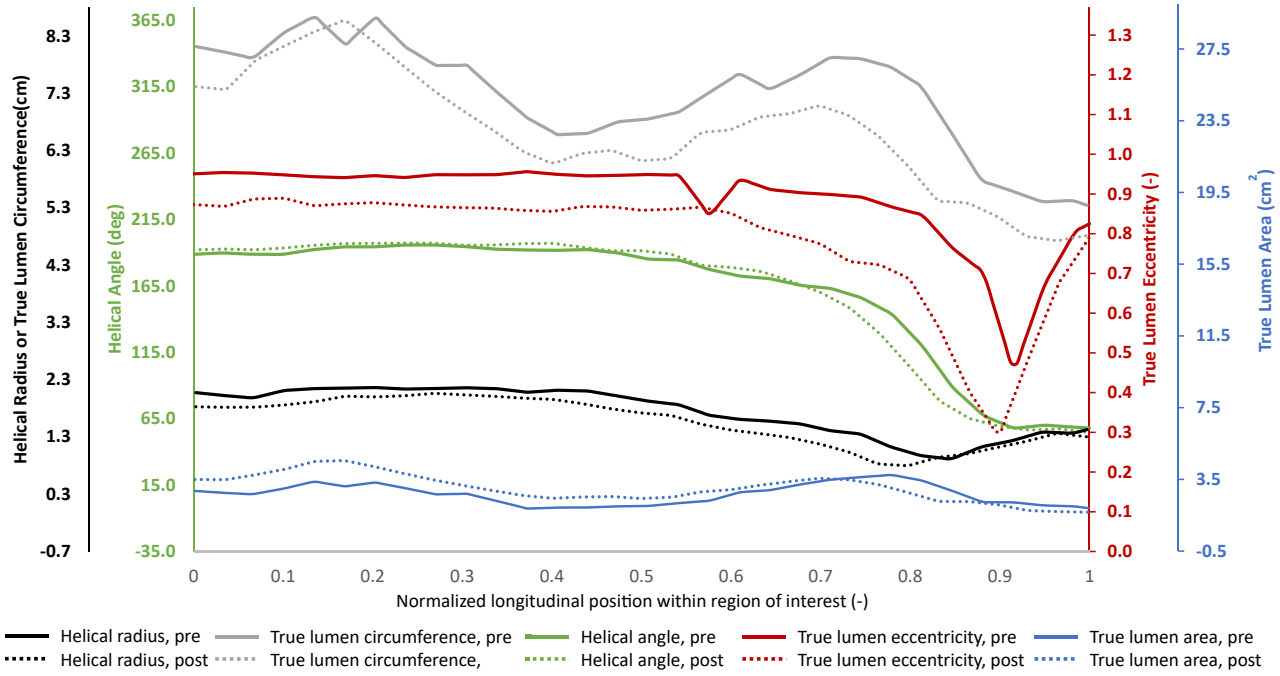

Fig 3. Longitudinal variation of helical radius, helical angle, and cross-sectional true lumen eccentricity, area, and circumference before (*solid lines*) and after thoracic endovascular aortic repair (TEVAR) (*dotted lines*). (*Top*) Example of an achiral acute dissection (A4). (*Bottom*) Example of a right-handed chiral chronic dissection (C1).

are angularly conformable, TEVAR may still decrease helical twist in some cases. This can be visualized in the altered probability density function of helical angle from before TEVAR (bimodal distribution) to after TEVAR (bell curve distribution) (Supplementary Fig, online only). The distribution change resulted mainly from two

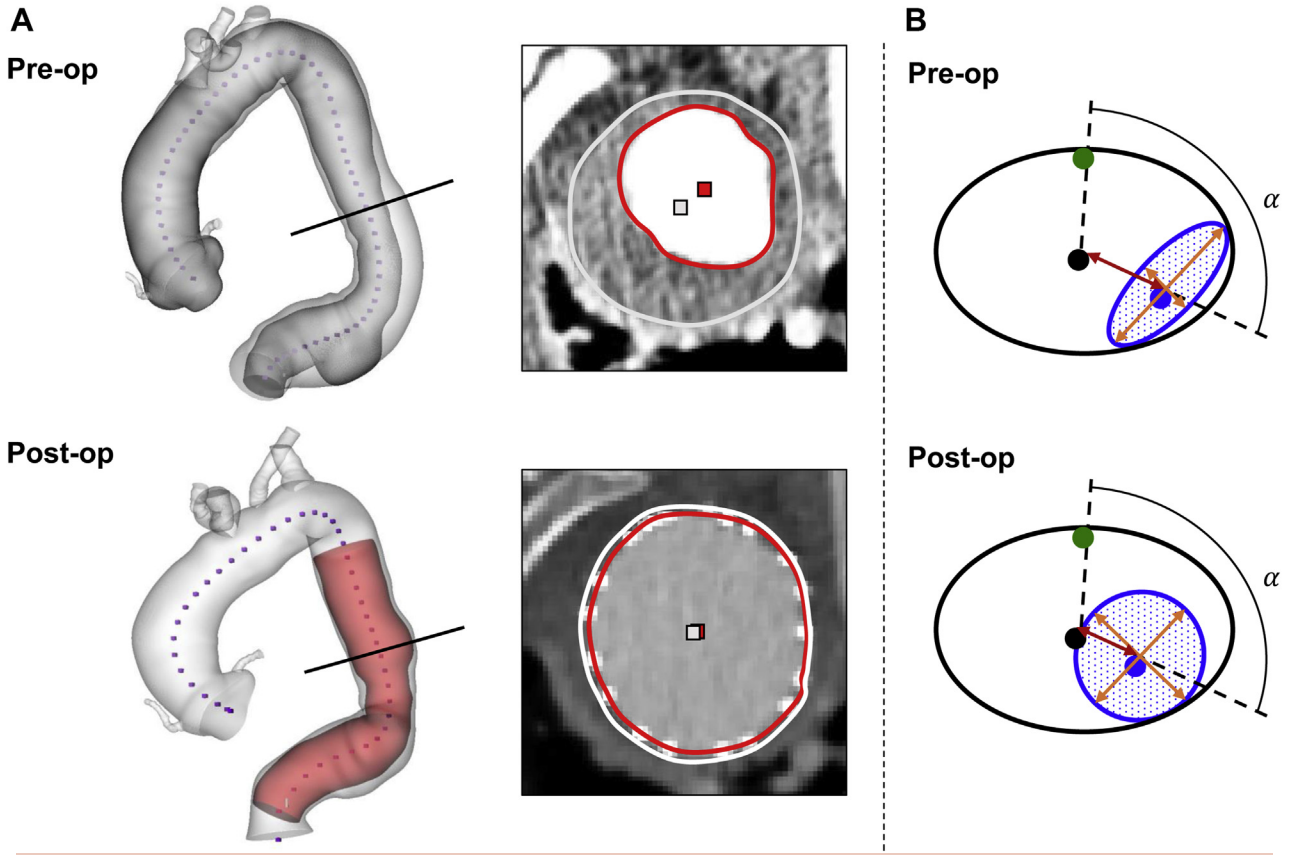

Fig 4. Visualization of morphological changes owing to thoracic endovascular aortic repair (TEVAR). **(A)** Surface models (*left column*) with axial slice locations (*black lines*), from which cross-sections (*right column*) were extracted for patient C4. Whereas the true lumen has relatively large area and low helical radius before TEVAR (*top row*), it expands into the whole aortic lumen while the false lumen is completed obliterated post-TEVAR (*bottom row*). Note that the centroids of the true lumen and whole aorta become essentially overlaid on each other post-TEVAR, not only decreasing the helical radius close to zero, but effectively eliminating helical morphology as well. **(B)** Illustration of TEVAR-induced changes on true lumen morphology in chronic dissections. Helical angle, α, and true lumen circumference (*blue line*) exhibit no changes, whereas helical radius (*red arrows*) and true lumen eccentricity (*based on orange arrows*) decrease and true lumen cross-sectional area (*shaded blue*) increases.

patients (A5, C4) transitioning from right-handed chiral to achiral owing to TEVAR. What these two cases had in common were high true lumen peak helical twists, low helical radii, and high true lumen areas and circumferences before TEVAR, and relatively long follow-up times. The surface models and cross-sections for patient C4 demonstrates an expansion of the true lumen into the whole aortic lumen while the false lumen diminishes (Fig 4, *A*). This means that TEVAR may affect effective helical morphology just by expanding the true lumen cross-section, especially with longer remodeling periods.

The patient cohort, as well as all subgroups, experienced a straightening of the true lumen corkscrew shape after TEVAR as evidenced by significantly decreased helical radius. Despite other helical metrics remaining unaltered, this theoretically produces a better environment for flow throughput since a straight flow lumen is advantageous when pressure gradients are more than 22.67 mm Hg in idealized pipe geometries.[20] The decrease of helical radius is a direct consequence of the true lumen cross-section expanding and having its centroid translate toward the centroid of the whole aortic lumen, all owing to false lumen depressurization. This notion is supported by the significant decrease in true lumen eccentricity and increase in true lumen area.

Even though vascular resistance mainly depends on the peripheral resistance (with about two-thirds of the resistance in the arterioles), we know that altered expanded cross-sections of large vessels can still lead to lower vascular resistance and more favorable conditions for blood flow. This is because, in the absence of downstream peripheral resistance, the blood flow rate is proportional to the fourth power of lumen diameter as governed by Poiseuille's law.[21] When the true lumen is dramatically compressed, as is the case in many patients with aortic dissection, there is a large capacity of cross-sectional

area expansion, especially for acute dissections. This is evident in the more than two-fold increase in true lumen area in the acute dissection patients from before to after TEVAR (3.0 cm^2 vs 6.4 cm^2), whereas the patients with chronic dissection experienced a much smaller expansion (3.0 cm^2 vs 4.3 cm^2) (Table II). The more dramatic true lumen area increase in acute dissections is a consequence of increasing lumen circumference as well as decreased eccentricity. This finding is likely due to a pliable intimal flap that has not yet stiffened.

In contrast, the patients with chronic dissection exhibited no change in the lumen circumference as a result of TEVAR; however, they exhibited significantly decreased eccentricity and increased area. It has been shown that, for ellipses with a fixed circumference, the optimal cross-sectional shape for flow is circular.[22] Interestingly, although the patients with chronic dissection as a whole exhibited stable circumference and increased area, the four chronic cases with follow-up time of less than 30 days showed no increase in the true lumen area and a significant decrease in the true lumen circumference. This outcome was likely a consequence of the endograft lining the intraluminal surface of the true lumen, acutely occupying luminal space with endograft wall thickness, especially in the presence of wrinkled graft material in an oversized endograft.[23] Over time, as the self-expanding stents exert radial outward force on the intraluminal surface, the true lumen expands and becomes more circular, as was shown in the whole chronic dissection subgroup. This hypothesis goes in line with the reported volumetric remodeling for one of the patients with a 12 month follow-up time in the chronic subgroup (C6).[24]

Theoretically, superposition of these four concepts: (1) straighter (decreased helical radius), (2) larger (increased cross-sectional area), (3) more circular (decreased eccentricity), and (4) pliable (increased circumference) true lumen all optimize fluid flow by decreasing impedance. As seen in the acuity subgroup data, acute dissections on all four fronts with TEVAR, whereas chronic dissections only benefit from the first three with sufficient remodeling time (Fig 4, *B*). In fact, the precise mixture of TEVAR-induced changes of dissection morphology may potentially be used as an indicator of dissection maturity and extent of pathologic remodeling.

There are some limitations and proposed future work related to this study. A larger patient cohort will be needed to reinforce these findings, especially with respect to the acuity and chirality subgroup analyses. Multiple follow-up time points could help to discern between immediate and long-term effects of TEVAR with regard to the helical and cross-sectional metrics, as was recently done with focus on luminal volumes and intimal tear location and size.[25] Although this cohort only included Gore C-TAG devices, other designs may induce different changes to dissection morphology. Also, considering that excessive oversizing can cause increased lumen narrowing, increase the risk for retrograde dissection at the proximal landing zone,[26] and that aggressive distal oversizing increases the need for reinterventions,[27] a future study is proposed to investigate the regions close to the endograft ends. The aims of this project are to refine oversizing recommendations for TEVAR and to predict complication risks based on preoperative morphology and device design and dimensions. Additionally, further generalization of the methodology would allow for analysis of type A dissections as well as multichannel dissections and, as a part of this generalization, TEVAR for patients with prior proximal repair could be studied more closely. Finally, because other studies have showed that dissection flap morphology depends on luminal pressures and that endografts influence pulse pressure and vessel compliance,[28,29] dynamic dissection image analysis could provide more biomechanics insights on flow lumen morphology.

CONCLUSIONS

Although TEVAR for type B aortic dissections does not significantly uncurl the corkscrew shape of the true lumen, it improves the flow boundary conditions by straightening the lumen path and making the cross-section larger and more circular. Additionally, for acute dissections, the true lumen also increases in cross-sectional circumference. These improvements can be explained by depressurization of the false lumen through coverage of the intimal tear, and the implantation of oversized, cylindrical devices that exert outward radial force and possess bending stiffness into the true lumen. The distinct bimodal grouping of right-handed chiral and achiral type B aortic dissections pre-TEVAR vanishes after intervention owing to favorable remodeling of some patients. This study provides evidence of TEVAR-induced changes to the helical morphology of type B aortic dissections, which may assist in intervention planning, device selection, outcome assessment, the development of devices better suited for dissection pathologies.

AUTHOR CONTRIBUTIONS

Conception and design: JB, GS, MD, JL, CC
Analysis and interpretation: JB, GS, JL, CC
Data collection: JB, GS, NM, MD, JL, CC
Writing the article: JB, GS, JL, CC
Critical revision of the article: JB, GS, NM, MD, JL, CC
Final approval of the article: JB, GS, NM, MD, JL, CC
Statistical analysis: JB, CC
Obtained funding: Not applicable
Overall responsibility: CC

REFERENCES

1. Nauta FJH, Trimarchi S, Kamman AV, Moll FL, van Herwaarden JA, Patel HJ, et al. Update in the management of type B aortic dissection. Vasc Med 2016;21:251-63.
2. Riambau V, Böckler D, Brunkwall J, Cao P, Chiesa R, Coppi G, et al. Editor's choice — management of descending thoracic aorta diseases. Eur J Vasc Endovasc Surg 2017;53:4-52.
3. Fanelli F, Dake MD. Standard of practice for the endovascular treatment of thoracic aortic aneurysms and type B dissections. Cardiovasc Intervent Radiol 2009;32:849-60.
4. Swee W, Dake MD. Endovascular management of thoracic dissections. Circulation 2008;117:1460-73.
5. Frolich MM, Suh G-Y, Bondesson J, Lee JT, Dake MD, Leineweber M, et al. Thoracic aortic geometry correlates with endograft bird-beaking severity. J Vasc Surg 2020;72:1196-205.
6. Bondesson J, Suh G-Y, Lundh T, Dake MD, Lee JT, Cheng CP. Quantification of true lumen helical morphology and chirality in type B aortic dissections. Am J Physiol Heart Circ Physiol 2021;320(2):H901-11.
7. Cheng A, Dagum P, Miller DC. Aortic root dynamics and surgery: from craft to science. Phil Trans R Soc B 2007;362:1407-19.
8. Gasser TC, Ogden RW, Holzapfel GA. Hyperelastic modelling of arterial layers with distributed collagen fibre orientations. J R Soc Interface 2005;3:15-35.
9. Suh G-Y, Beygui RE, Fleischmann D, Cheng CP. Aortic arc vessel geometries and deformations in patients with thoracic aortic aneurysms and dissections. J Vasc Interv Radiol 2014;25:1903-11.
10. Ullery BW, Suh G-Y, Hirotsu K, Zhu D, Lee JT, Dake MD, et al. Geometric deformations of the thoracic aorta and supra-aortic arch branch vessels following thoracic endovascular aortic repair. Vasc Endovasc Surg 2018;52:173-80.
11. Hirotsu K, Suh G, Lee JT, Dake MD, Fleischmann D, Cheng CP. Changes in geometry and cardiac deformation of the thoracic aorta after thoracic endovascular aortic repair. Ann Vasc Surg 2018;46:83-9.
12. Suh G, Ullery BW, Lee JT, Dake MD, Fleischmann D, Cheng CP. Cardiopulmonary-induced deformations of the thoracic aorta following thoracic endovascular aortic repair. Vascular 2019;27:181-9.
13. Wilson N, Wang K, Dutton RW, Taylor CA. A software framework for creating patient specific geometric models from medical imaging data for simulation based medical planning of vascular surgery. Lecture Notes in Computer Science 2001;2208:449-56.
14. Bondesson J, Suh G-Y, Lundh T, Lee JT, Dake MD, Cheng CP. Automated quantification of diseased thoracic aortic longitudinal centerline and surface curvatures. J Biomech Eng 2020;142:041007. (9 pages).
15. Lundh T, Suh G-Y, Digiacomo P, Cheng CP. A Lagrangian cylindrical coordinate system for characterizing dynamic surface geometry of tubular anatomic structures. Med Biol Eng and Comput 2018;56:1659-68.
16. Choi G, Cheng CP, Wilson NM, Taylor CA. Methods for quantifying three-dimensional deformation of arteries due to pulsatile and nonpulsatile forces: implications for the design of stents and stent grafts. Ann of Biomed Eng 2009;37:14-33.
17. Snedecor GW, Cochran WG. Statistical methods. 8 ed. Ames, IA: Iowa State University press; 1989.
18. Khoynezhad A, Toluie S, Al-Atassi T. Treatment of the chronic type B aortic dissection: the pro-endovascular argument. Semin Thorac Cardiovasc Surg 2017;29:131-6.
19. Lou X, Chen EP, Duwayri YM, Veeraswamy RK, Jordan WD Jr, Zehner CA, et al. The impact of thoracic endovascular aortic repair on long-term survival in type B aortic dissection. Ann Thorac Surg 2018;105:31-9.
20. Jinsou Z, Benzhao Z. Fluid flow in helical pipe. Acta Mech Sin 1999;15:299-312.
21. Hall JE. Guyton and Hall Textbook of Medical Physiology. 13 ed. Philadelphia, PA: Elsevier; 2016.
22. Lekner J. Viscous flow through pipes of various cross-sections. Eur J Phys 2007;28:521-7.
23. Parodi JC, Ferreira LM, Faella H, La Mura R, Ruslender E, Henestrosa G. Use of stents and endograft as a rescue treatment in a patient with a complex form of recurrent aortic coarctation. J Vasc Surg 2007;45:1263-7.
24. Suh G-Y, Hirotsu K, Beygui RE, Dake MD, Fleischmann D, Cheng CP. Volumetric analysis demonstrates that true and false lumen remodeling persists for 12 months after thoracic endovascular aortic repair. J Vasc Surg Cases 2016;2:101-4.
25. Sun W, Xu H, Xiong J, Li Z, Chen Y, Yang G, et al. 3D morphologic findings before and after thoracic endovascular aortic repair for type B aortic dissection. Ann Vasc Surg 2021. Pre-proof ahead of print, published online Jan 25, 2021.
26. Liu L, Zhang S, Lu Q, Jing Z, Zhang S, Xu B. Impact of oversizing on the risk of retrograde dissection after TEVAR for acute and chronic type B dissection. J Endovasc Ther 2016;23:620-5.
27. Jang H, Kim M-D, Kim G-M, Won JY, Ko Y-G, Choi D, et al. Risk factors for stent graft-induced new entry after thoracic endovascular aortic repair for Stanford type B dissection. J Vasc Surg 2017;65:676-85.
28. Bäumler K, Vedula V, Sailer AM, Seo J, Chiu P, Mistelbauer G, et al. Fluid-structure interaction simulations of patient-specific aortic dissection. Biomech Model Mechanobiol 2020;19:1607-28.
29. Nauta FJH, de Beaufort HWL, Conti M, Marconi S, Kamman AV, Ferrara A, et al. Impact of thoracic endovascular repair on radial strain in an *ex vivo* porcine model. Eur J Cardiothorac Surg 2017;51:783-9.

Submitted Dec 18, 2020; accepted Apr 19, 2021.

Additional material for this article may be found online at www.jvascsurg.org.

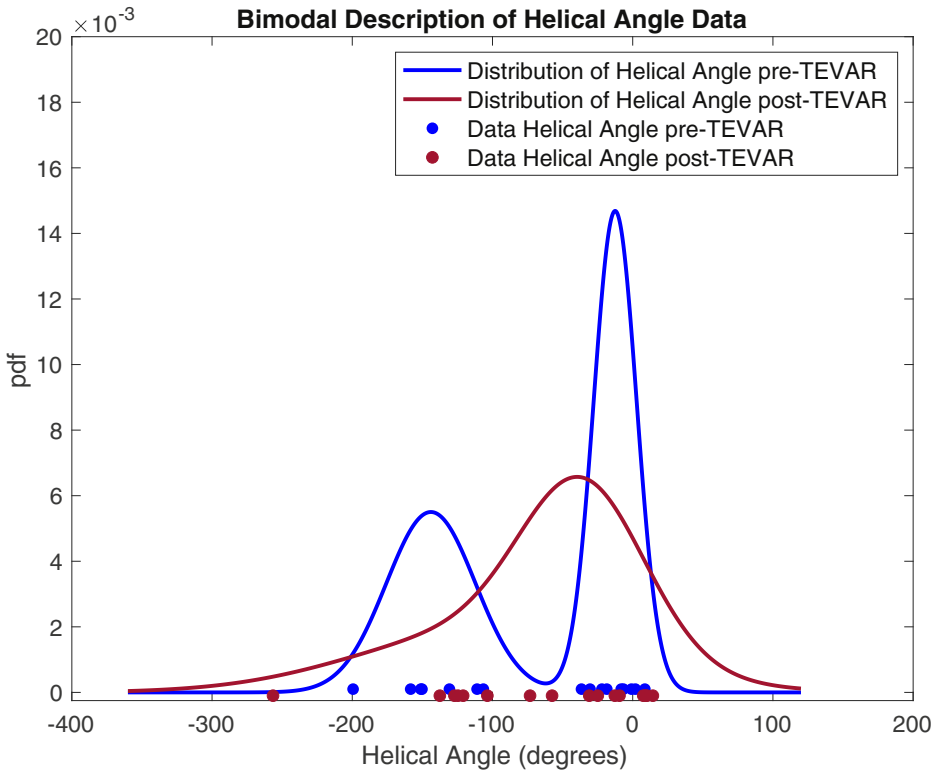

Supplementary Fig (online only). Probability density function (*pdf*) visualizing how the chirality subgroups are distinctly bimodal before thoracic endovascular aortic repair (*TEVAR*) (*blue*), but not distinct after TEVAR (*red*).